Available online at www.sciencedirect.com
ScienceDirect
Journal of Magnetic Resonance 187 (2007) 327–342
JMR Journal of Magnetic Resonance
www.elsevier.com/locate/jmr

Methods for peak assignment in low-resolution multidimensional NMR cross-correlation relaxometry

N. Marigheto [a], L. Venturi [a,b], D. Hibberd [a], K.M. Wright [a], G. Ferrante [a,c], B.P. Hills [a,*]

[a] *Institute of Food Research, Norwich Research Park, Colney, Norwich NR4 7UA, UK*
[b] *Department of Food Science, University of Bologna, Italy*
[c] *Stelar srl., Via E.Fermi 4, 27035 Mede (PV), Italy*

Received 24 January 2007; revised 29 March 2007
Available online 18 May 2007

Abstract

Several NMR protocols are presented for assigning peaks in complex T_1–T_2 spectra, including the effects of varying the spectrometer frequency and the CPMG pulsing rate. Extensions into a third dimension based on chemical-shift; diffusion- and field-cycled weighted T_1–T_2 cross-correlation methods are also explored as a means of peak assignment. We illustrate the power of these novel techniques with reference to simple aqueous sucrose solutions, but the methodology should be generally applicable.

Keywords: NMR relaxometry; Cross-correlation; Peak assignment; Sucrose

1. Introduction

Low-resolution time-domain NMR relaxometry has found wide application as a non-invasive tool for determining oil and water contents, pore size distributions in porous materials and phase changes associated, for example, with changing solid–liquid ratios, polymer gelation and aggregation. Such determinations can be undertaken on low-field, low-cost bench-top NMR spectrometers operating at frequencies typically less than 25 MHz. These measurements are usually based on the simple Free Induction Decay (FID); the Carr-Purcell-Meiboom-Gill (CPMG) and Inversion (or saturation) recovery pulse sequences. In many applications the magnetisation decay (or recovery) data are inverse Laplace transformed into a continuous 1-dimensional distribution of transverse or longitudinal relaxation times (a ''relaxation time spectrum'') and examples abound in the literature [1].

More recently NMR relaxometry has made an important advance with the advent of a fast algorithm for 2-dimensional inverse Laplace inversion [2]. This has given rise to ''multidimensional'' relaxometry which is somewhat analogous to the extension of 1-dimensional high-resolution NMR spectra into multidimensional spectroscopy in the frequency domain. Several papers have appeared exploring the potential of multidimensional relaxometry for characterising porous rocks [3], complex processed foods such as cheese [4,5] egg and cake [6] and intact cellular plant tissue [7,8] none of which are readily amenable to analysis with conventional high resolution NMR spectroscopy. Such 2-dimensional spectra contain far more information than conventional 1-dimensional relaxation time spectra. Even an apparently simple sample such as a gelatine gel gives rise to at least eight distinct peaks in the T_1–T_2 spectrum (unpublished results). Such high information content presents many opportunities for sample characterisation but also makes it difficult to assign the peaks to particular proton pools. It is therefore necessary to step back from the complexities of real multiphase, multicomponent systems and see to what extent the multidimensional spectra of ''model'' single-component solutions can be interpreted. As we shall see, assigning the 2-dimensional peaks in even simple sucrose solutions is far from straight-

* Corresponding author. Fax: +44 1603 507723.
E-mail address: Brian.Hills@bbsrc.ac.uk (B.P. Hills).

1090-7807/$ - see front matter © 2007 Elsevier Inc. All rights reserved.
doi:10.1016/j.jmr.2007.04.016

forward especially when there is the possibility of proton exchange and magnetisation transfer. In this paper we therefore explore various NMR protocols for T_1–T_2 peak assignment, choosing sucrose solutions as the test system.

Although sucrose solutions have been chosen because of their simplicity, they are, nevertheless of considerable commercial importance. The binding of sugars to enzymes and other environment-sensitive biopolymers is being explored as a possible means of their preservation and sugar glasses are being developed for controlled drug delivery and flavour encapsulation. For this reason, several groups have investigated the molecular dynamics of sucrose solutions. High resolution ^{13}C relaxometry has been used to measure the motional correlation times of individual carbon atoms in sucrose [9]. This has shown that the $-CH_2OH$ group labelled 6f in Fig. 1 is the most rotationally labile while those labelled 1f and 6g are sterically hindered. Recent molecular dynamics simulations [10] indicate that sucrose in aqueous solution most likely exhibits internal flexibility around the glycosidic linkage. Indeed a 2-D Roesy study of sucrose in supercooled water gave evidence for a transient inter-residue hydrogen bond between the oxygens 2g and 1f in Fig. 1 [11]. Moreover all the solid-state intramolecular hydrogen bonds are replaced with hydrogen bonds to surrounding water molecules. Most recently, molecular dynamic simulations [12] suggest that the sucrose conformation is stabilised by two inter-residual, bridging water molecules between oxygens labelled 2g and 3f as well as 2g and 1f. Nevertheless the exchange lifetimes of these bridging water molecules are sub-picoseconds so for present purposes they can be included in the pool of exchangeable water. A fast field-cycling study of aqueous sucrose systems has been reported [13] and showed that the sucrose correlation time in the saturated solution is of the order of 10–20 ns at 298 K. It is interesting to note that this earlier study found no evidence of multiple exponential longitudinal relaxation and successfully fitted the data as a single exponential. This highlights the power of multidimensional T_1–T_2 relaxometry because, as we shall see, there are actually (at least) four peaks with different T_1's. It would therefore be interesting to measure the frequency-dependence of the T_1–T_2 sucrose spectrum on a field-cycling spectrometer and this possibility is explored in a later section.

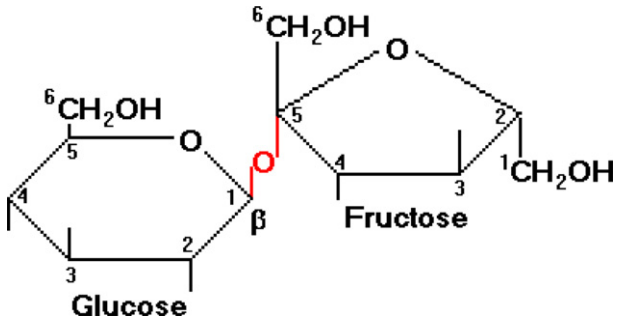

Fig. 1. A schematic molecular model of sucrose.

2. Materials and methods

NMR measurements were performed on aqueous sucrose solutions thermostated at 295 K using Resonance Instruments DRX spectrometers operating at either 23.4, 100 or 300 MHz. Field-cycling T_1–T_2 measurements were undertaken at Stelar srl. in Mede (PV), Italy. The pulse sequences have been described elsewhere [2–6]. The T_2-store-T_2 sequence was undertaken with full phase cycling. In particular, $+M_z$ and $-M_z$ were added during the store period to minimise the effects of longitudinal relaxation during the store period. The data were analysed with a MATLAB script incorporating the fast 2-D inverse Laplace transform algorithm [2]. The default value (unity) of the regularisation parameter was used in the inversion algorithm.

3. Theoretical analysis of proton exchange effects in T_1–T_2 spectra

3.1. Analytical predictions

An unexpected feature of many T_1–T_2 cross-correlation spectra, including those of sucrose solutions, is the appearance of low-intensity peaks in a "forbidden" region where $T_1 < T_2$. On first consideration it is tempting to dismiss such peaks as artefacts of the 2D-Inverse Laplace transformation process and this remains a possibility. However in some samples the peaks are reproducible even when the regularisation parameter in the transformation is iterated and optimised. If the peaks are real they could be an interesting consequence of proton exchange. The role of 2-site magnetisation transfer, either by proton exchange or secular dipolar interactions, in T_1–T_2 spectra has been explored by Hills et al. [6] and most recently by McDonald et al. [17,18]. If the two exchanging sites are labelled a and b, then under intermediate exchange conditions four peaks are predicted at the corners of a square at locations (s_1^+, s_2^+), (s_1^+, s_2^-), (s_1^-, s_2^+) and (s_1^-, s_2^-) where

$$s_i^{+/-} = -0.5(R_{ai} + k_{ai} + R_{bi} + k_{bi}) \pm 0.5[(R_{ai} + k_{ai} + R_{bi} + k_{bi})^2 - 4((R_{ai} + k_{ai})(R_{bi} + k_{bi}) - k_{ai}k_{bi})]^{1/2} \quad (1)$$

are the effective relaxation rates.

Similar calculations have been made for the T_2-store-T_2 sequence [18] where the variable store period allows exchange of longitudinal magnetisation. These calculations show that in T_2-store-T_2 spectra slow 2-site exchange at short storage times only two peaks on the diagonal appear close to the intrinsic T_{2a} and T_{2b}. In the fast exchange regime only a single peak on the diagonal appears at the weighted average T_2. However, at intermediate exchange rates, comparable to the reciprocal storage time, two off-diagonal cross-peaks appear, thereby forming what could be called a symmetric "exchange square". We will show examples of such "exchange squares" in both T_2-store-T_2 and T_1–T_2

spectra. However, the exchange "square" in T_1–T_2 spectra are often found to be quite distorted rectangles and this is somewhat mystifying and complicates peak assignment. Of course the distortions could merely be the result of experimental imperfections and noise, but they might have a more significant origin. We therefore undertook a numerical simulation of the effects of 2-site exchange in T_1–T_2 spectra to see whether such distortions also arise theoretically.

3.2. Numerical simulations

A Monte–Carlo simulation was used to investigate the distortions of the "exchange square" in T_1–T_2 spectra. This Monte–Carlo simulation had already been developed in our laboratory to explore the combined effects of proton exchange and diffusion during the CPMG [14] and PGSE pulse sequences [15], so it was adapted to simulate 2-site exchange in the T_1–T_2 sequence.

The simulation is based on randomly distributing **S** magnetisation density vectors among N^3 volume elements in a cube. Each magnetisation vector is assigned a resonance frequency, transverse and longitudinal relaxation rate according to whether it is a water or sucrose hydroxyl proton. Proton exchange is introduced by ascribing a probability p_{mn} to each vector that it changes from chemical species m to n in one time step of the simulation. The total magnetisation after each time step is calculated by summing the individual magnetisation vectors taking into account their precession and relaxation. The effect of the T_1–T_2 pulse sequence is taken into account directly by introducing phase changes on the individual magnetisation vectors during the simulation. The specifically spatial aspects of these earlier simulations [14,15] were suppressed as domain structure or other types of spatial heterogeneity play no part in the present analysis. The simulation parameters listed in Table 1 were chosen to be appropriate to those of water protons exchanging with a single pool of sucrose hydroxyl protons in a 67% w/w saturated sucrose solution. Thus the water protons were assigned T_1 and T_2's of one second and the water and sucrose hydroxyl protons had an average chemical shift difference of 1.4 ppm, which was the value used in an earlier study [14]. The sucrose hydroxyl protons were considered to be a single proton pool and their intrinsic relaxation times were assumed to be close to the experimental values of the non-exchanging CH protons in a saturated sucrose solution, namely a T_1 of 30 ms and a T_2 of 10 ms. (see Fig. 3). The simulated effect of reducing the proton exchange rate from 1400 s^{-1} (the fast exchange regime) to 14.0 s^{-1} (an intermediate exchange regime) at a spectrometer frequency of 23.4 MHz with a 90–180° CPMG pulse spacing of 1 ms is shown in Fig. 2. It is remarkable that the single peak observed in the fast exchange limit splits into four distinct peaks in the T_1–T_2 spectrum under intermediate exchange conditions. It is particularly noteworthy that the off-diagonal cross-peaks do not lie on the corners of a square, and, as we shall show, this can be seen experimentally. However the origin of the distortions remains uncertain. The Monte–Carlo simulation has inherent noise resulting from random fluctuations in the magnetisation exacerbated by the small number (200) of spin vectors used in the simulation. This noise will result in deconvolution errors and could well explain the distortions. It was also found that the pattern of peak splitting is sensitive to the exact values of the exchange rate, proton fractions and intrinsic relaxation rates. Fig. 2c shows the "forbidden" peak vanishes merely by increasing the exchange rate from 14 to 23.35 s^{-1} and using a higher spectrometer frequency of 100 MHz. The absence of off-diagonal cross-peaks does not therefore imply there is no magnetisation exchange.

4. Results

4.1. T_1–T_2 spectra of saturated sucrose solutions

Fig. 3a shows the T_1–T_2 cross-correlation spectrum of a saturated sucrose solution at 299 K and having a pH of 8.15. This was acquired at a spectrometer frequency of 23.4 MHz with a CPMG 90–180° pulse spacing of 200 μs. Four peaks, labelled 1 through 4 are observed in the region where $T_1 > T_2$ (to the right of the diagonal dashed line). Assigning these peaks is far from straightforward. Some clues are obtained from the measured relative peak areas. A saturated sucrose solution has a concentration of ca 60% w/w which means that, if all the protons are NMR visible, 31% of the total peak area should correspond to non-exchanging sucrose CH protons and 69% to the pool of exchangeable hydroxyl protons of sucrose and water. Peak

Table 1
The parameters used in the computer simulation of the effects of proton exchange in a 2-site T_1–T_2 spectrum

Figure number	k	Spectrometer Frequency /MHz	del/ppm	CPMG tau/ms	Water/sucrose hydroxyl proton ratio
2a	1400	23.4	1.4	1	2.335
2b	14.01	23.4	1.4	1	2.335
2c	23.35	100	1.4	1	2.335
2d	0	23.4	0	0.5	2.335

k is the rate (s^{-1}) for the exchange of sucrose hydroxyl protons onto water.
del/ppm is the average chemical shift between sucrose and water hydroxyl protons.
CPMG tau, is the 90–180° pulse spacing assumed in the simulation.
The water protons were assigned intrinsic T_1 and T_2 values of 1 s. The sucrose hydroxyl protons were assigned intrinsic values of $T_1 = 30$ ms and $T_2 = 10$ ms.

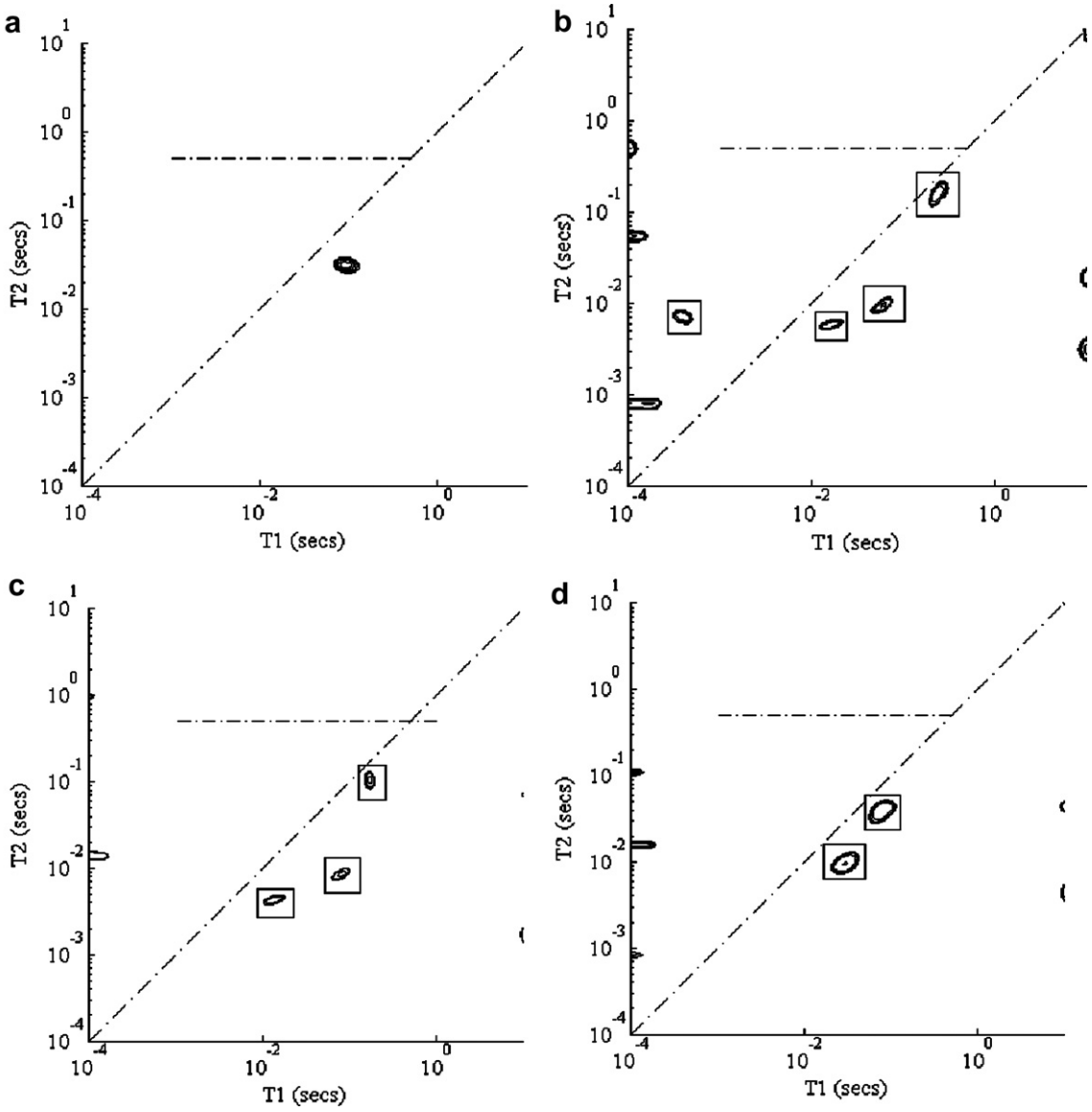

Fig. 2. Theoretical simulations of the effect of 2-site exchange between sucrose and water hydroxyl protons with the parameters listed in Table 1. (a) Fast exchange, (b and c) intermediate exchange, (d) no exchange.

1 in Fig. 2 has the longest T_1 and T_2 so undoubtedly arises from water protons, however its measured relative peak area is only 51.2% which suggests that peak 2, with a relative area of 8.8% may arise from slowly exchanging sucrose hydroxyl protons. Peaks 1 and 2 then have a combined area of 60%, which, while still short of the theoretical 69% for all exchangeable protons, is reasonably close, given experimental errors and the uncertainties incurred in the 2-dimensional inverse Laplace inversion operation. To try to confirm these provisional assignments both system and NMR parameters were varied systematically, beginning with the proton exchange rate.

4.1.1. Varying the proton exchange rate

It is known that the proton exchange rate in a saturated sucrose solution is greatly reduced compared to the dilute solution [18] so that peak 2 could well correspond to a separate sucrose hydroxyl proton peak in the slow-exchange regime. This possibility was tested by lowering the pH from 8.15 to 1.64 with addition of a trace of HCl to increase the exchange rate. If our assignment is correct than peaks 1 and 2 should merge under the resulting fast exchange conditions, Fig. 3b shows the results are somewhat ambiguous in that the peaks appear less well resolved and have merged into just two groups. Peak 1 in Fig. 3b now has a relative area of 58% which compares well with the sum of peaks 1 and 2 in Fig. 3a. The nature of peak 2 in Fig. 3a therefore remains uncertain but could arise from slowly exchanging sucrose hydroxyl protons. To progress further we consider variation of the spectrometer frequency.

4.1.2. Varying the main spectrometer frequency

Three spectrometers were available to us, operating at proton frequencies of 23.4, 100 and 300 MHz. Fig. 4b

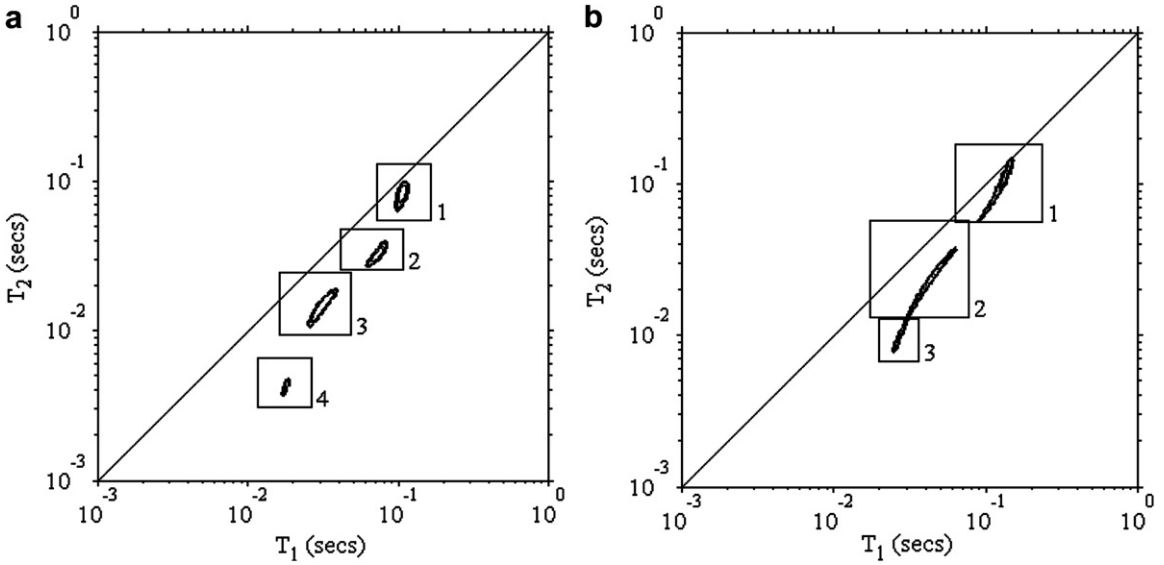

Fig. 3. The effect of exchange rate on the T_1–T_2 spectra of a saturated sucrose solution at 295 K acquired at 23.4 MHz with a CPMG pulse spacing of 200 μs. (a) Neutral pH 8.15, (b) pH 1.64.

shows the T_1–T_2 spectrum of the saturate sucrose solution at pH 8.15 acquired at the higher spectrometer frequency of 300 MHz with a short CPMG pulse spacing of 200 μs. It can be seen that the T_1's of all the peaks are shifted to higher values. However peaks 2, 3 and 4 in Fig. 4a shift much more in the T_1 dimension than peak 1, suggesting that they arise from non-exchanging protons. This follows because, in the fast proton exchange the relaxation rate $1/T_1$ of peak 1 is the weighted average of the intrinsic relaxation rates of the hydroxyl protons on water and sucrose. While the T_1 of the sucrose hydroxyl proton is expected to increase with spectrometer frequency that of the water, which dominates the average, will not because it is motionally narrowed. On the other hand the reduction in the spectral density at higher frequencies means that peaks arising from the non-exchanging sucrose CH proton pools should shift to much longer T_1 values. In contrast, the dependence of the intrinsic T_2's on spectrometer frequency is much weaker so only small shifts are seen. Fig. 4b shows that, because of the T_1 shifts peaks 1,2 and 3 are no longer resolved. As expected, very similar results are seen at pH 1.64 (Fig. 4c and d). Taken together these observations again suggest, somewhat indirectly, that, at least peaks 3 and 4 in Fig. 3a arise from non-exchanging sucrose protons, but this assignment and the nature of peak 2 remains uncertain. We therefore proceeded to the next variable, namely the CPMG pulsing rate.

4.1.3. Varying the CPMG pulsing rate

The exchanging and non-exchanging proton pools can, in principle, be distinguished by decreasing the CPMG pulsing rate at high spectrometer frequency. This follows because the dephasing rate of the exchanging hydroxyl proton pool increases with decreasing pulsing rate and increasing spectrometer frequency as a consequence of the chemical shift difference between the water and sucrose hydroxyl protons [1]. This contrasts with the behaviour of the non-exchanging proton pools whose dephasing rate should be independent of CPMG pulsing rate, provided there is no dephasing by diffusion through field inhomogeneities. Fig. 5a and b show the effect of decreasing the CPMG pulsing rate (or equivalently, increasing the 90–180 pulse spacing, tau) at 100 and 300 MHz, respectively, at pH 8.15. In agreement with these predictions, the $T_2$of the dominant exchangeable proton peak 1 decreases dramatically with increasing pulse spacing in both cases while that of peak 2 is unchanged. This strongly suggests that peak 2 in Fig. 3a arises not from hydroxyl protons but from non-exchanging sucrose CH protons. Peak 3 in Fig. 4b and d corresponding to non-exchanging protons cannot be seen because the CPMG pulse spacing is too long.

4.1.4. Varying the sucrose concentration

The high viscosity of saturated sucrose solutions not only shortens the proton relaxation times it also reduces the proton exchange rate. It is therefore of interest to compare the saturated spectra with those of a more dilute sucrose solution. Fig. 6a shows the T_1–T_2 spectrum for a 15% w/w sucrose solution acquired at room temperature at 23.4 MHz with a CPMG pulse spacing of 400 μs. The faster proton exchange rate in this more dilute regime (earlier work suggests exchange rates of the order of 10^3 s^{-1}) means that all the exchangeable protons appear as a single high-intensity (93.7%) peak (labelled 1 in Fig. 6a) at long T_1 and T_2. What is particularly noteworthy is that peaks 2, 3 and 4 of the saturated sucrose solution (see Fig. 3a) have shifted to longer T_2 but have also become more separated in the T_1 dimension suggesting that their motional correlation times have not only all been reduced but are now significantly different. This is consistent with their

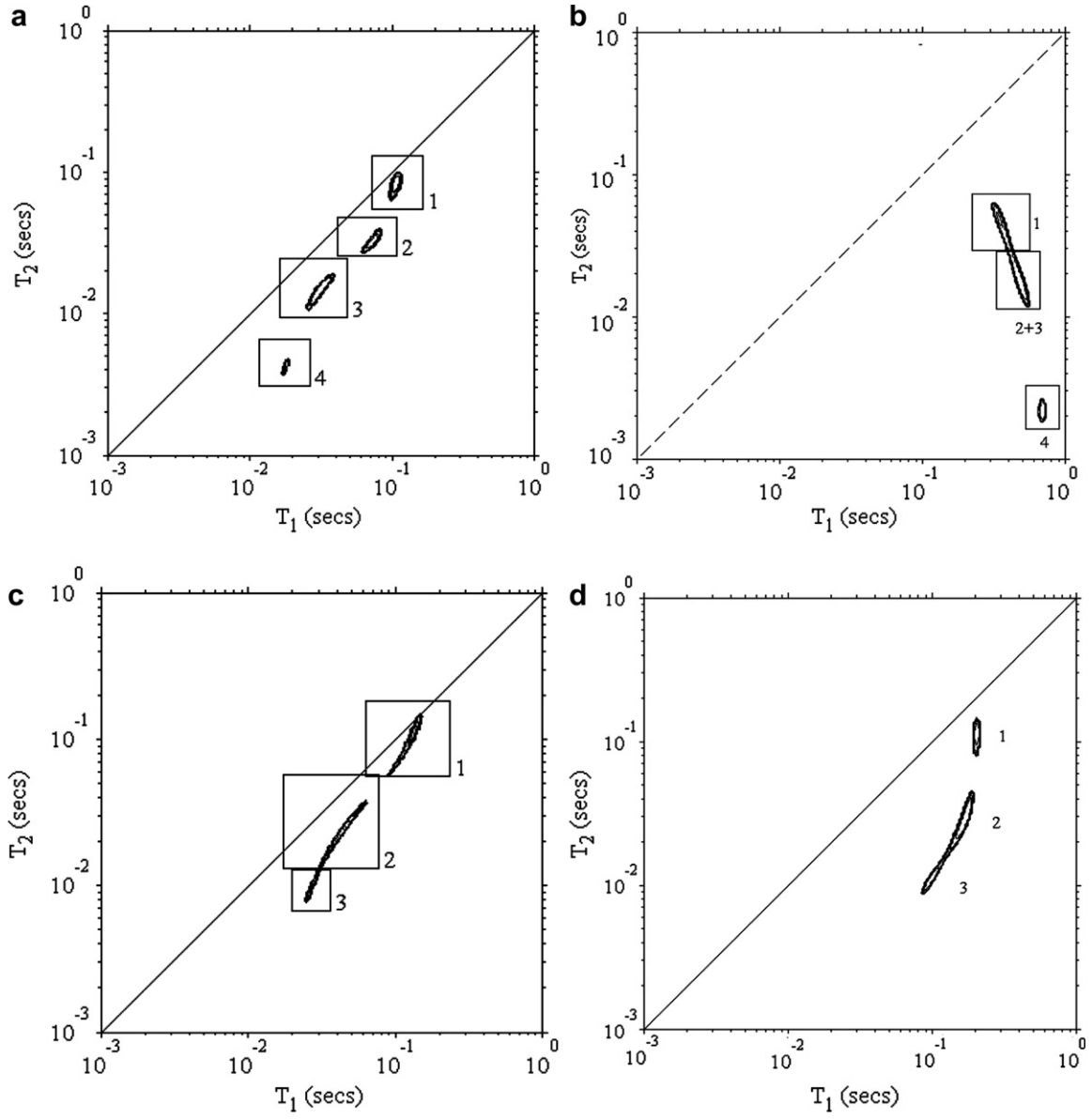

Fig. 4. The effect of spectrometer frequency on the T_1–T_2 spectra of a saturated sucrose solution at 295 K, with a CPMG pulse spacing of 200 μs. (a) 23.4 MHz, pH 8.15; (b) 300 MHz, pH 8.15; (c) 23.4 MHz, pH 1.64; (d) 100 MHz, pH 1.64.

assignment to different sucrose CH protons. The effect of lowering the exchange rate by reducing the temperature to 278 K is particularly interesting and results in the single exchangeable proton peak (peak 1 in Fig. 6a) splitting into several well-resolved peaks (Fig. 6b). Unfortunately the assignment problem arises again, because it is unclear which of the peaks has arisen from the exchangeable protons. The combined intensity (90%) of peaks 1 and 2 in 6b compares well with that of the fast exchange peak in Fig. 6a (91%). It is also probable that the peaks labelled 5 and 6 in Fig. 6b corresponds to peaks 3 and 4 in Fig. 6a, though this remains uncertain.

Despite these uncertainties the observation that peaks 3 and 4 in Fig. 6b lie in the "forbidden" zone where $T_1 < T_2$ suggest that they arise from intermediate proton exchange as predicted by the theoretical simulations in Section 2 and this strengthens the case that forbidden peaks are not an artefact of the 2-D inverse Laplace transformation but result from real exchange processes.

4.1.5. Replacing water with D_2O

The sucrose spectra presented so far have been dominated by the high intensity exchangeable proton peak which is mainly water. This has made it harder to reliably characterise the remaining low-intensity non-exchanging proton peaks. It is therefore of interest to suppress the water peak. In this section we do this simply by replacing H_2O with D_2O but this substitution is not practical with many samples, such as processed foods, so more general ways for suppressing the water signal in T_1–T_2 spectra will

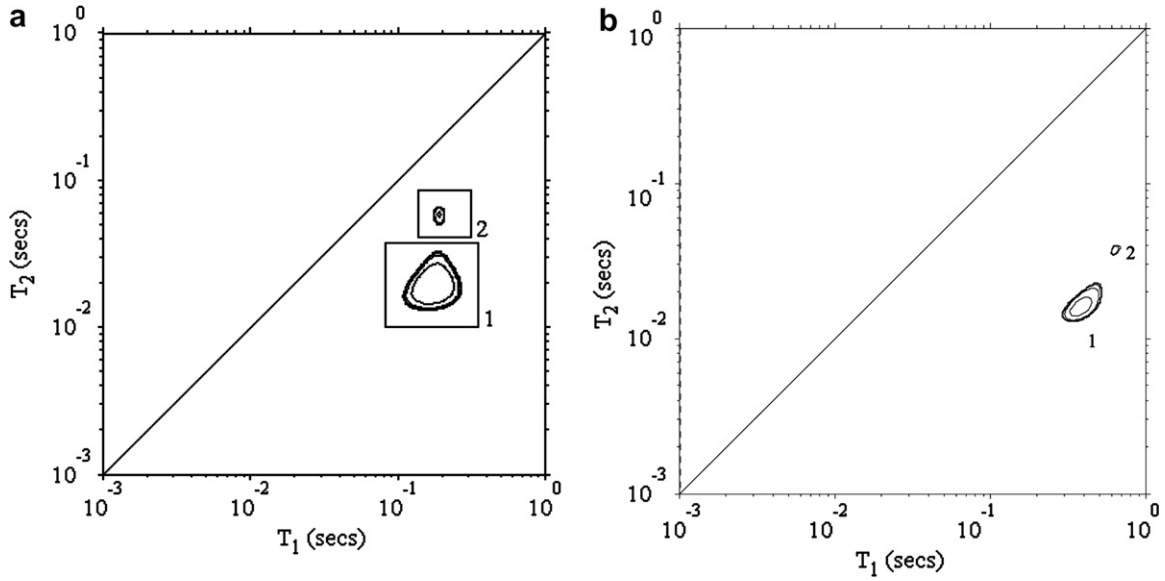

Fig. 5. The effect of increasing CPMG pulse spacing on the T_1–T_2 spectra of a saturated sucrose solution at 295 K, pH 8.15 (a) 100 MHz tau 4 ms (b) 300 MHz tau 1 ms.

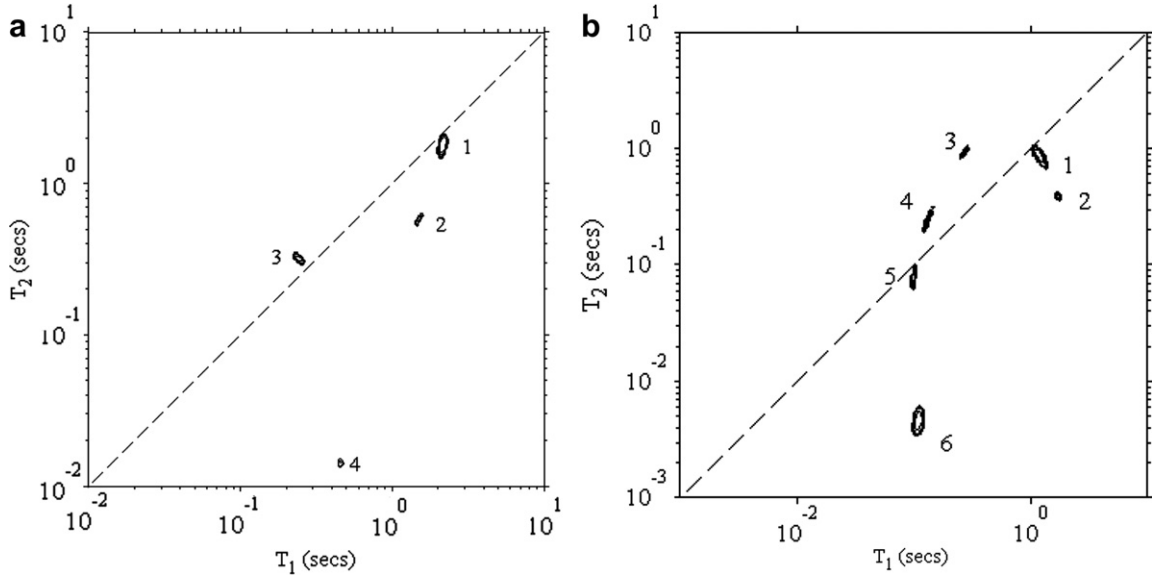

Fig. 6. The T_1–T_2 spectrum of a 15% w/w/ sucrose solution in H_2O. (a) 298 K at 23.4 MHz. (b) 278 K at 100 MHz.

be presented in Section 4.2 Fig. 7 shows the spectra of a 15% w/w sucrose solution in D_2O acquired at a proton frequencies of 23.4 and 100 MHz. The peak labelled 1 in Fig. 7a has roughly equal T_1 and T_2 values of about 3 s, so this undoubtedly arises from residual HOD and this implies that the remaining peaks 2, 3 and 4 in Fig. 7a arise from non-exchanging sucrose CH protons. They also correspond reasonably well to peaks 2, 3 and 4 in Fig. 6a, which supports their assignment to CH proton pools. The corresponding spectrum at 100 MHz (Fig. 7b) has been included because it illustrates many of the complexities of cross-correlation spectroscopy. Peaks 1 and 2 in Fig. 7b undoubtedly correspond to the CH sucrose peaks 2 and 3 in Fig. 7a, however new peaks (6–9) have appeared at very long T_1's at 100 MHz. These are poorly characterised by the inverse Laplace algorithm and are therefore best regarded as artefacts arising from a failure to properly characterise the long T_1 component of HOD. Great care must therefore be taken in the inversion process. The same can be said for the very short T_2 components. Peak 5 is undoubtedly an artefact as its T_2 is comparable to the CPMG pulse spacing. But peak 4 at 23.4 MHz has now split into two distinct peaks (3 and 4) at 100 MHz.

4.2. The extension to 3-dimensions

The previous section showed that peak assignment can be greatly assisted by varying parameters such as the pro-

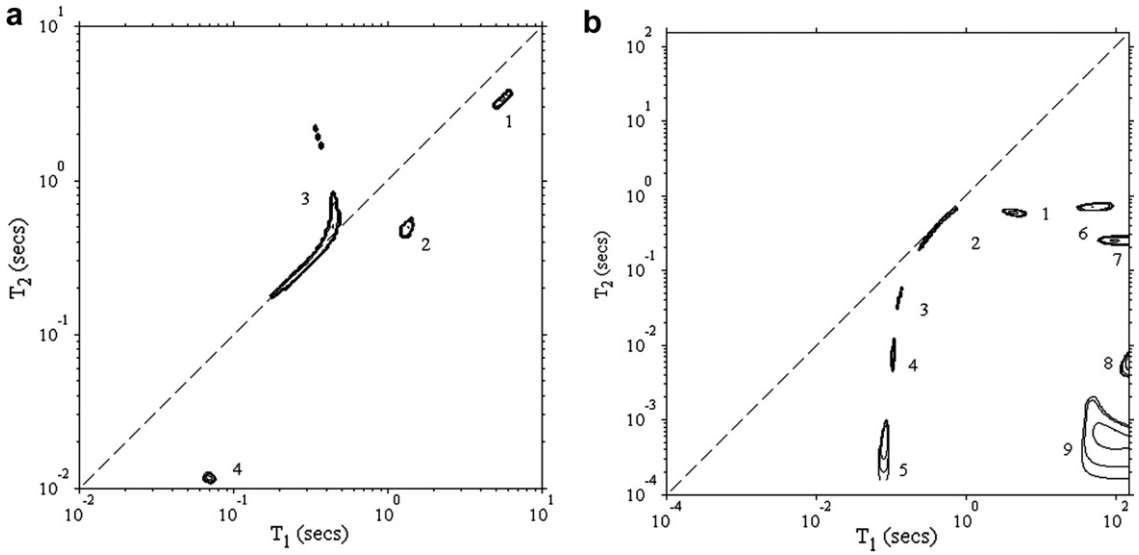

Fig. 7. The T_1–T_2 spectrum of a 15% w/w/ sucrose solution in D_2O at 298 K. (a) 23.4 MHz (b) 100 MHz.

ton exchange rate, the spectrometer frequency and CPMG pulsing rate and by replacing H_2O with D_2O. This has shown that peaks 2–4 in Fig. 3a) of the saturated solution and peaks 2–4 in the dilute 15% solution arise from non-exchanging sucrose CH protons. Nevertheless, more detailed assignment remains uncertain and it is not always possible to vary the proton exchange rate or to add D_2O without destroying or irreversibly changing the sample. In this section we therefore explore the potential for extending cross-correlation relaxometry to a third dimension. In other words, creating a set of 2-dimensional spectra ''stack-plotted'' in the third dimension as a function of a third independent variable. We explore three possibilities for this variable, namely the chemical shift, the wavevector, q, and the spectrometer frequency. Each will be considered in turn.

4.3. Chemical-shift resolved T_1–T_2 spectra

In principle the sucrose peaks could all be assigned by acquiring the T_1–T_2 spectra at high frequency on a high resolution NMR spectrometer. Fourier transformation of the echo decay envelopes from each spin-echo of the CPMG sequence would then yield a frequency spectrum and allow chemical shift separation of the non-exchanging sucrose peaks. A separate T_1–T_2 spectrum could then be obtained for each chemically-resolved peak in the proton frequency spectrum. This has been done for simple oil–water peaks in cheese [4] where different emulsion microphases have different chemical shifts but it has yet to be attempted on single phase systems such as sucrose where there are more subtle intramolecular proton chemical shifts. Fig. 8 shows the frequency spectrum of a 20% w/w sucrose solution in D_2O acquired on our DRX300 spectrometer at 300 MHz by Fourier transforming a single spin echo. Separate peaks are resolved and can be assigned on the basis of earlier work [16]. Unfortunately the spectral resolution in Fig. 8 is not particularly good because the spectrometer was not set up for high resolution work and lacked sample spinning facilities. Nevertheless separate T_1–T_2 spectra could be extracted from the 3D-data set for each of the highlighted points in the spectrum in Fig. 8. In most cases each spectral peak gave rise to single peaks in the T_1–T_2 spectrum although the lower number of points acquired in the time domains resulted in shifts in the T_1–T_2 peak positions compared to the better resolved 2-dimensional T_1–T_2 spectrum. In this way a number of the peaks could be provisionally assigned in the 300 MHz T_1–T_2 spectrum (see Fig. 9a). Curiously the (G5, F5) spectral peak contributed to two different peaks in the T_1–T_2 spectrum. While this high resolution NMR protocol succeeds in assigning the sucrose peaks at 300 MHz, this does not solve the assignment problem because it remains uncertain which peak at 300 MHz corresponds to which peak at lower spectrometer frequency, as a comparison of the spec-

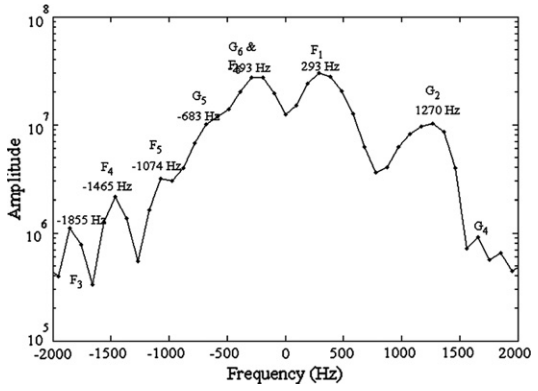

Fig. 8. The high resolution spectrum of a 20% sucrose solution in D_2O acquired at 300 MHz from a spin echo at 298 K without sample spinning. Peak assignments are shown (see also Fig. 1).

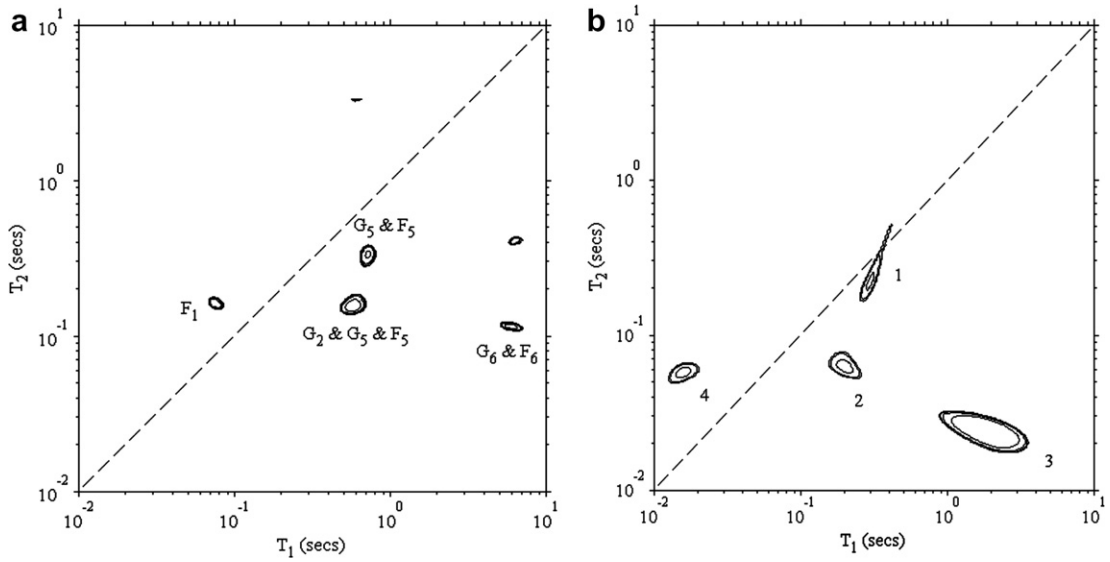

Fig. 9. (a) The T_1–T_2 spectrum of a 20% sucrose solution in D_2O at 298 K acquired at 300 MHz. The main peaks have been assigned from the separate T_1–T_2 spectra acquired from each peak in Fig. 8. (b) The corresponding spectrum in H_2O.

tra at 23.4 MHz (Fig. 6a) and 300 MHz (Fig. 9a) reveals. Nor is it always possible to acquire chemical shift resolved spectra on more complex, heterogeneous biopolymer systems, such as food. For comparison the T_1–T_2 spectrum of 20% sucrose in H_2O has been included (see Fig. 9b). Peaks 1–3 correspond to the assigned sucrose CH peaks in Fig. 9a but, in addition, we now have a dominant water peak (peak 3) at short T_2.

4.4. q-Weighted T_1–T_2 spectra

The T_2–D spectrum of a 20% sucrose solution at 23.4 MHz has already been reported [7] and, as expected, comprises two peaks, one for sucrose CH protons centred on ($T_2 = 376$ ms and $D = 1.97.10^{-10}$ m^2 s^{-1}) and the other for the exchangeable proton pool ($T_2 = 1309$ ms and $D = 9.26.10^{-10}$ m^2 s^{-1}). The observation that the sucrose self-diffusion coefficient is about 5 times less than that of the exchangeable proton pool suggests that acquiring diffusion-weighted T_1–T_2 spectra in a 3-dimensional experiment would be another useful assignment tool. The diffusion weighting is most easily introduced by inserting a PGSE step at the start of the CPMG. If the pulsed gradient area, q, is progressively increased at constant echo time, TE, and the gradient pulse separation, Δ, then this becomes a (t_1, t_2, q^2) experiment in which the amplitude of each relaxation time peak i, is attenuated by the factor $\exp(-q^2 D_i \Delta - TE/T_{2i})$ where $D_i$is the effective, unrestricted diffusion coefficient of the protons associated with peak i. A log plot of the peak amplitudes against q^2 will therefore yield the effective diffusion coefficient for each peak. For the sucrose system there are only two diffusion coefficients so it is sufficient to acquire T_1–T_2 spectra for only a few discrete q values. Because water has the highest diffusion coefficient this also provides a simple means of acquiring water-suppressed T_1–T_2 spectra, which is especially useful in high water-content samples where the water peak dominates more interesting solute peaks.

Fig. 10 shows the effect of increasing the PGSE gradient amplitude on the T_1–T_2sucrose spectra of a 20% solution measured at 23.4 MHz. The percentages in Fig. 10 show the relative integrated area of the water peak and show the extent of the water suppression. Fig. 11 shows the dependence of the peak intensity for peaks 1 and 4 on $q^2\Delta$. The slopes of the plots give effective diffusion coefficients of $1.38{\cdot}10^{-9}$ and 5.97×10^{-10} m^2 s^{-1}, respectively, which are in reasonable agreement with those measured in the T_2–D spectrum for water and sucrose. This 3-dimensional q^2-weighted T_1–T_2 protocol, in combination with the T_2–D spectrum, is therefore a useful assignment tool which is more generally applicable that the high resolution chemical shift method of the previous section.

4.5. Field-cycled T_1–T_2 spectra

Conventional field-cycling NMR uses field-switching to measure the dispersive-dependence of T_1 on spectrometer frequency and such dispersions directly probe the spectral density functions giving rise to the longitudinal relaxation and, in simple cases, permit the correlation times of the molecular processes contributing to the relaxation to be extracted [17]. By implementing the T_1–T_2 pulse sequence on a fast field cycling relaxometer it is possible to generate a 3-dimensional stacked-plot of T_1–T_2 spectra where the spectrometer frequency forms the third dimension. In the field-cycled versions of the T_1–T_2 spectrum each peak should exhibit its own characteristic frequency dispersion, thereby identifying the spectral density function(s) contributing to it which not only assists in peak assignment but, more generally, helps resolve peaks that overlap at high

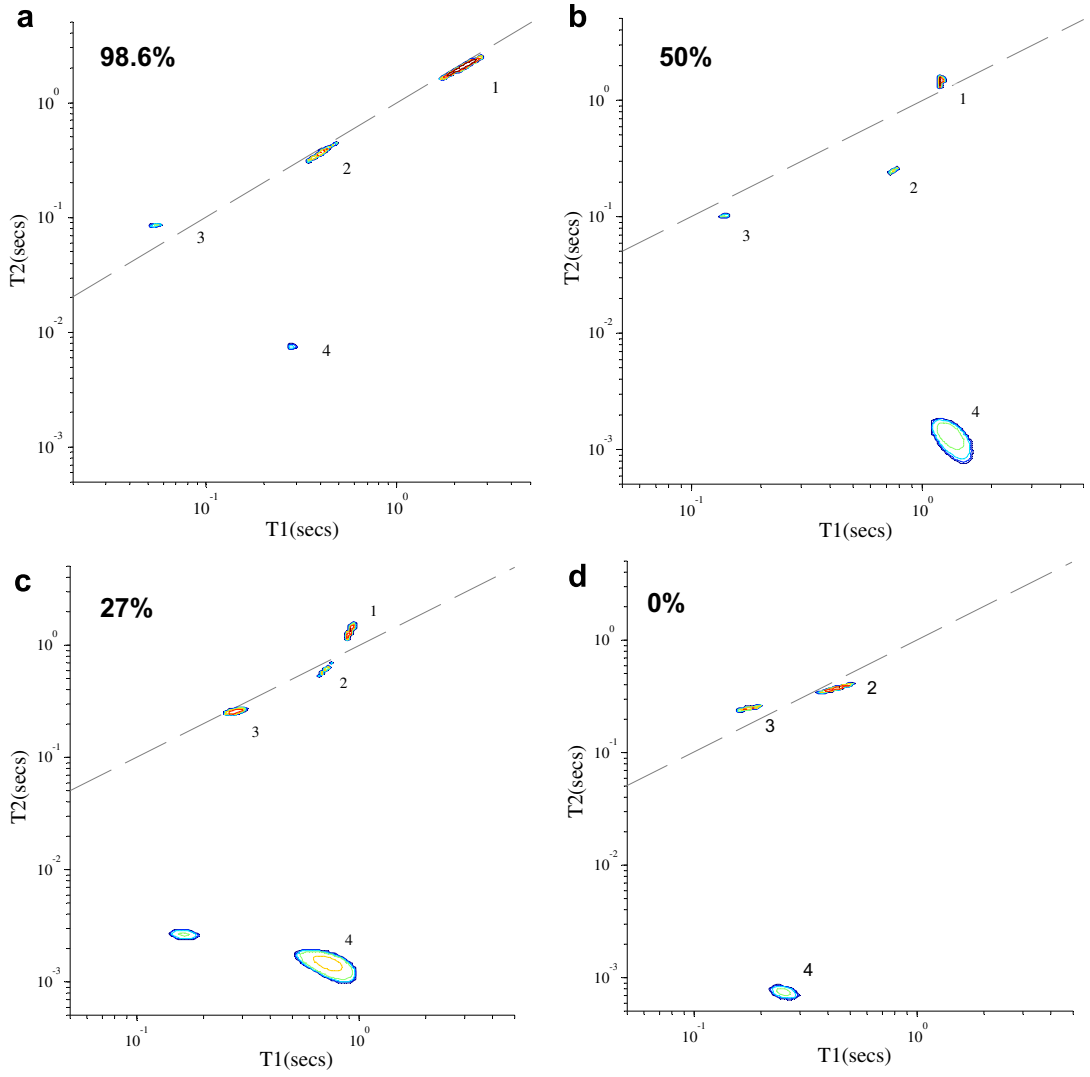

Fig. 10. q-weighted T_1–T_2 spectra of a 20% sucrose solution at 298 K acquired at 23.4 MHz in H_2O. (a) The T_1–T_2 spectrum without gradients. (b) Water suppression to a peak percentage of 50%. (c) Water suppression to a percentage of 27%. (d) Complete water suppression.

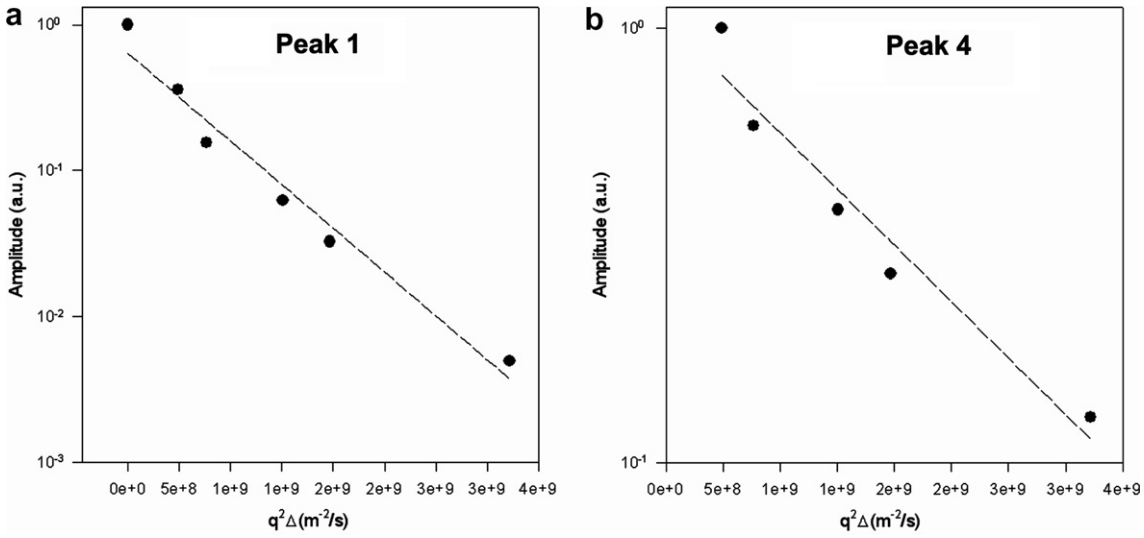

Fig. 11. The dependence of the T_1–T_2 peak intensities in Fig. 10 on gradient strength (q^2) for (a) peak 1 and (b) peak 4. The effective diffusion coefficients extracted from the slopes are (a) 1.38×10^{-9} m^2 s^{-1} and (b) 5.97×10^{-10} m^2 s^{-1}.

frequency.The field-cycling can be implemented during the inversion recovery and/or the CPMG dimensions depending on the type of information required. Fig. 12a shows the field-cycling version of the T_1–T_2 pulse sequence where the field cycling is only implemented during the inversion recovery step. Fig. 12b shows how it is also possible to implement field-cycling during a CPMG sequence in either the T_1–T_2 or T_2-store-T_2 sequences. Of course it is also possible to field cycle the store period in the T_2-store-T_2 sequence and this would show the frequency-dependence of the cross-relaxation longitudinal mixing process.

Fig. 13a–d show representative T_1–T_2 spectra acquired on a Stelar fast field-cycling relaxometer at relaxation fields of 0.1, 1, 2 and 4 MHz. while the CPMG step is undertaken at the fixed frequency of 8 MHz and Fig. 14 shows the frequency dispersions for the three principle relaxation peaks. The experimental point at 0.1 MHz is of questionable reliability, nevertheless the results establish, for the first time, that it is possible to measure 2-dimensional cross-correlation T_1–T_2 spectra on a fast field-cycling relaxometer and thereby extend the measurement into the third (frequency) dimension.

5. T_2-store-T_2 spectra

Provided the store time is short compared with longitudinal magnetisation transfer times, the T_2-store-T_2 spectrum has no off-diagonal cross-peaks and comprises only peaks along the diagonal. A comparison of the T_2-store-T_2 spectrum at very short store times with the corresponding T_1–T_2 spectrum can therefore help identify exchange peaks in the T_1–T_2 spectrum. In particular, a peak in the T_1–T_2 spectrum that does not appear on the diagonal at the same T_2 in the T_2-store-T_2 spectrum is most probably

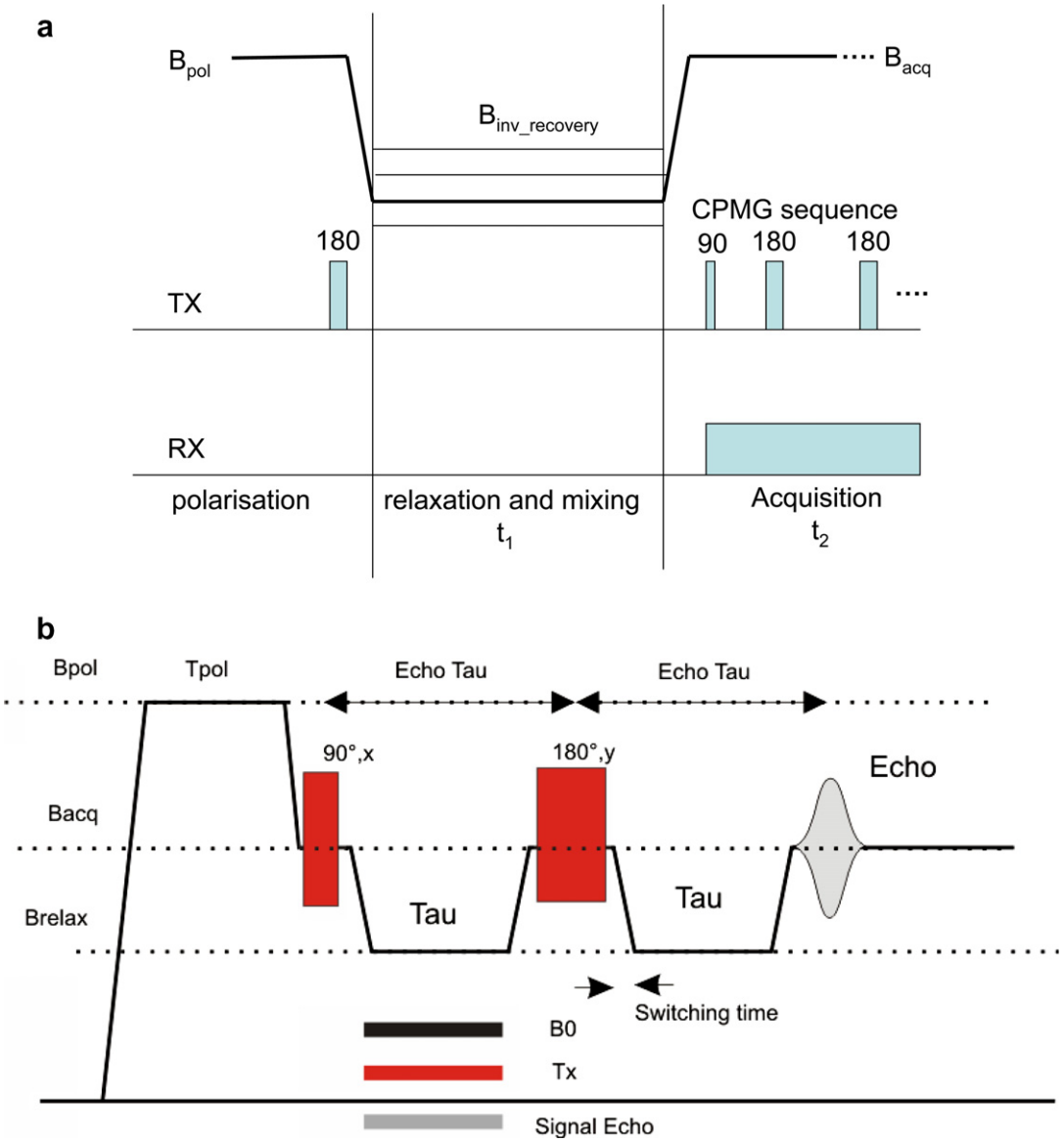

Fig. 12. (a) The 3-D field-cycling T_1–T_2 pulse sequence used to acquire the data in Fig. 13. (b) The field-cycled version of the CPMG pulse sequence.

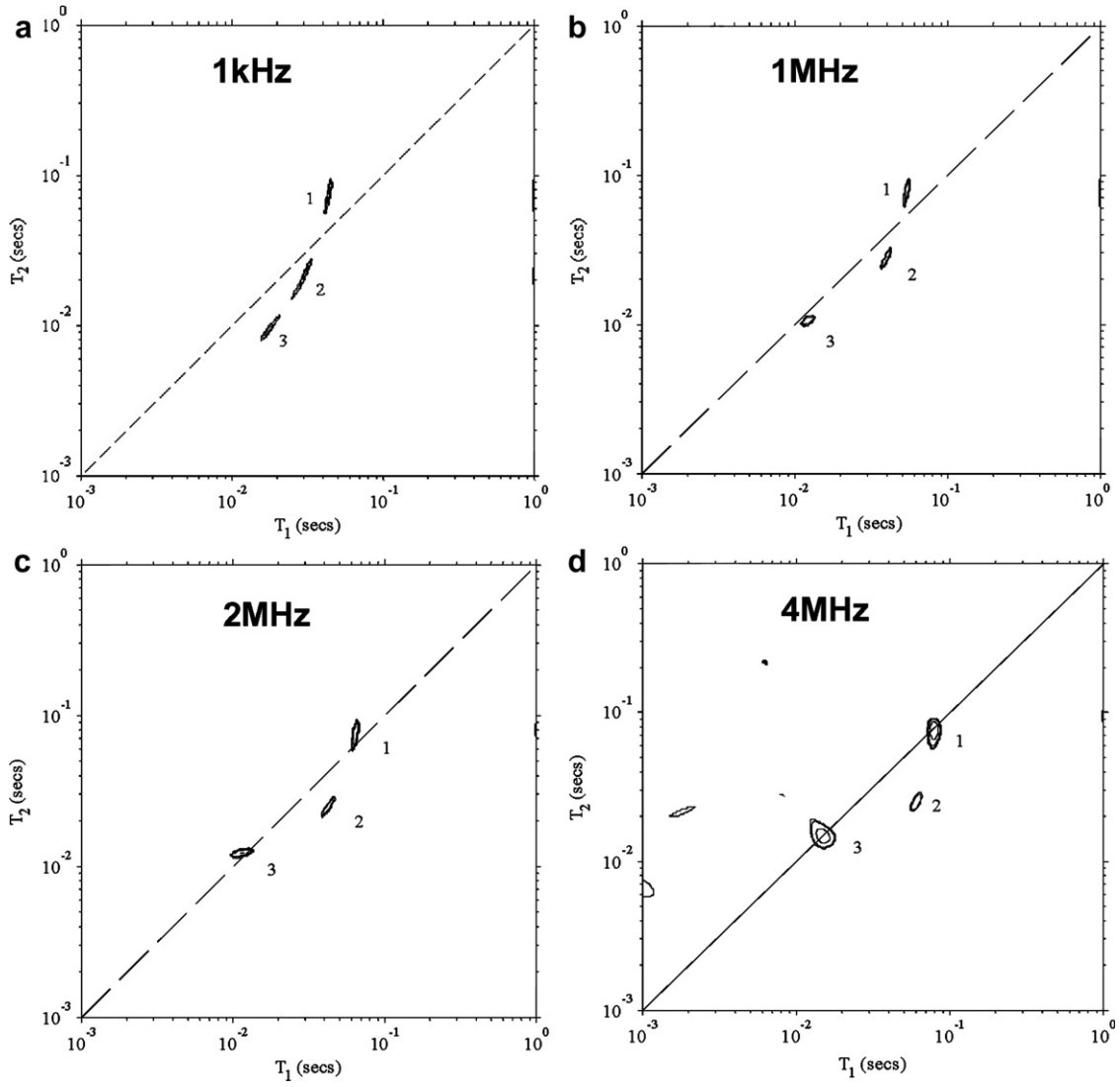

Fig. 13. Representative field-cycled T_1–T_2 spectra acquired when the t_1 dimension was recovering in the indicated relaxation fields (see Fig. 12). (a) 100 kHz. (b) 1 MHz. (c) 2 MHz. (d) 4 MHz.

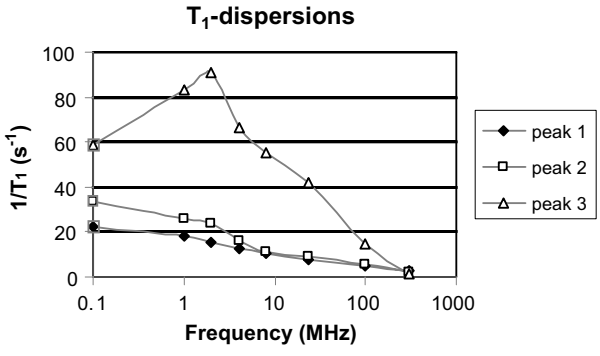

Fig. 14. The frequency dispersions of T_1 derived from the indicated peaks in the field-cycled T_1–T_2 spectra discussed in Fig. 13.

an exchange peak. In a similar way, a comparison of the T_2-store-T_2 spectrum in H_2O and D_2O, does, in theory, eliminate proton exchange cross-relaxation pathways leaving only secular dipolar cross-relaxation.

5.1. T_2-store-T_2 spectra of a saturated sucrose solution in H_2O and D_2O

Fig. 15a shows the T_2-store-T_2 spectrum of a saturated sucrose solution in H_2O acquired at 23.4 MHz with a short store time of 200 μs and a CPMG 90–180° spacing of 200 μs. No off-diagonal cross-peaks are seen at such short store times and the diagonal peaks correspond to those labelled 1–4 in Fig. 3a, confirming that all four peaks are intrinsic and not exchange cross-peaks. Peak 4 is poorly characterised because only 85 points were acquired in the first time dimension to avoid excessively long acquisition times. Increasing the store time to 2 ms introduces three off-diagonal cross-peaks (Fig. 15b) which can be assigned with the assumption that they lie on the corners of

exchange squares. We use the nomenclature that CP*ij* is the cross-peak between diagonal peaks *i* and *j* and the cross-peak on the opposite corner of the square is then CP*ji*. The observation of off-diagonal cross-peaks implies that the effective exchange lifetime of the proton magnetisation is of the same order of magnitude as the store time, namely ca. 2 ms. The absence of peaks in the opposite corners of the squares is presumably a consequence of their low intensity. Increasing the store time to 12 ms (Fig. 15c) causes CP_{32} to be replaced by CP_{23} while increasing the store time to 40 ms (Fig. 15d) merely causes the cross-peaks to begin to merge together.

Fig. 16a shows the corresponding set of spectra in D_2O. At a long store time of 40 ms the spectrum resembles Fig. 15a and shows three peaks along the diagonal with the same T_2's. The intensity of peak 1 is reduced from 66% in H_2O to 48% in D_2O so undoubtedly arises from HOD. The percentages of peaks 2 and 3 have both increased showing that they arise from non-exchanging sucrose CH protons. Curiously, however, as the store time is reduced below 1 ms exchange cross-peaks appear between peaks 1 and 2, though the exchange square is quite distorted. Also there is a hint of a cross-peak between peak 3 and 4, though this is very close o the diagonal, so could represent a genuine sucrose CH peak. The emergence of exchange peaks on the sub-millisecond timescale in the saturated solution is surprising and must show the efficiency of the secular dipolar interactions in this very viscous material. The exchange "square" between peaks 1 and 2 is more clearly seen in the corresponding T_1–T_2 spectrum in D_2O (Fig. 17).

5.2. T_2-store-T_2 spectra of a 20% w/w sucrose solution in H_2O and D_2O

Fig. 18a shows the T_2-store-T_2 spectrum of a 20% sucrose in H_2O acquired at 23.4 MHz with a short store time of 200 μs. As expected, the four peaks observed in

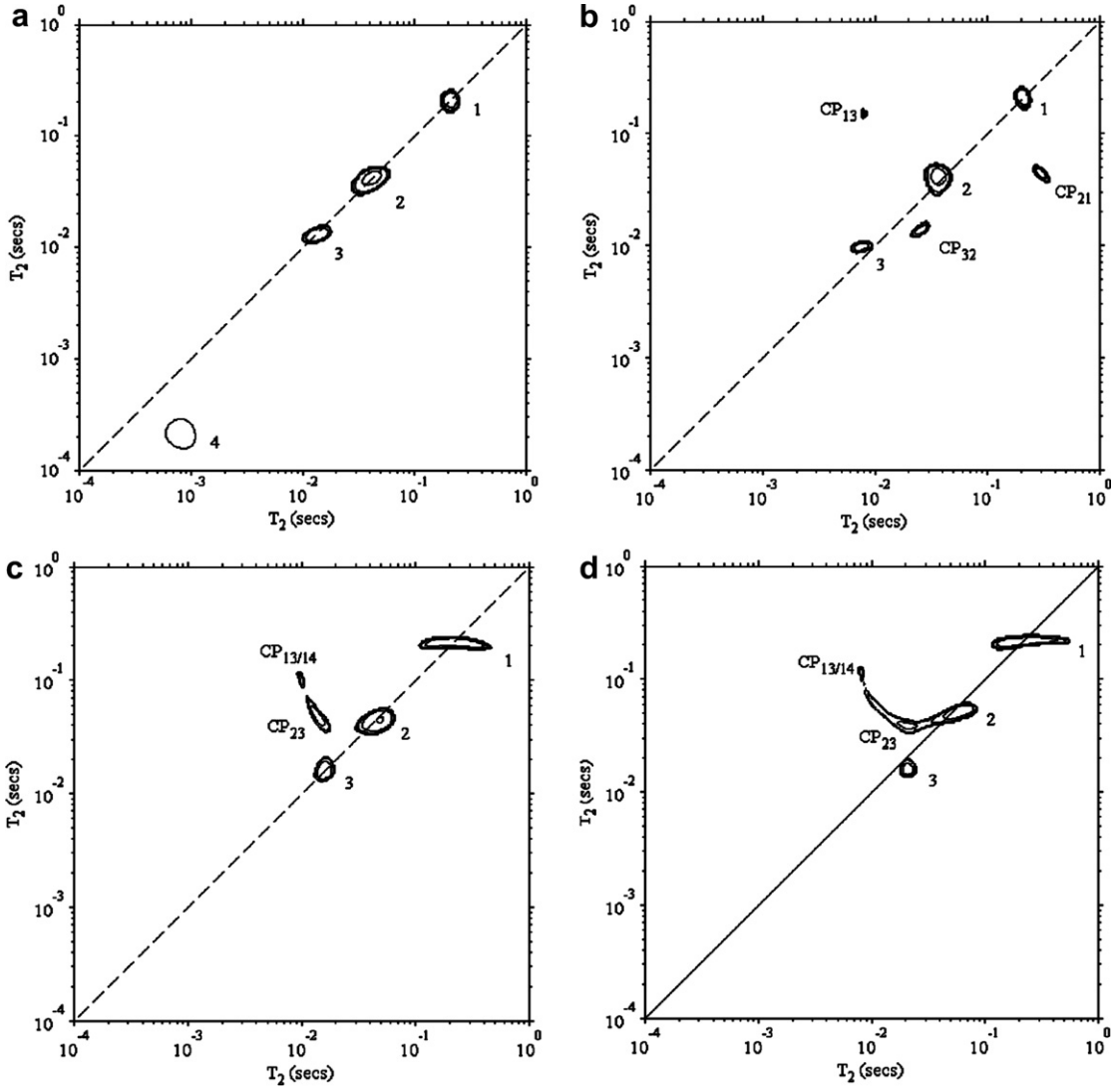

Fig. 15. T_2-store-T_2 spectra of saturated sucrose in H_2O acquired at 23.4 MHz with a CPMG pulse spacing of 200 μs and store times of (a) 200 μs; (b) 2 ms; (c) 12 ms; (d) 40 ms.

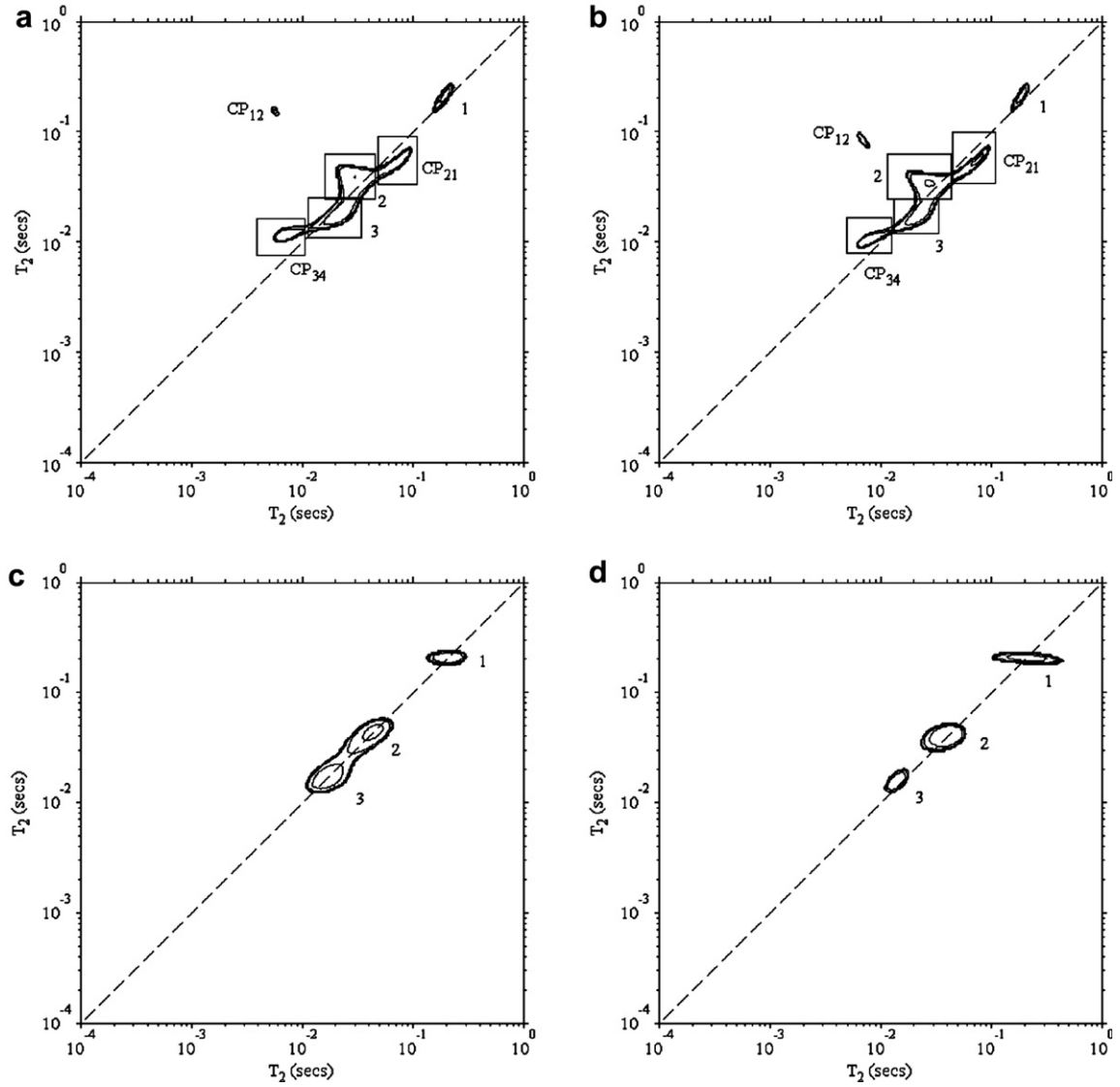

Fig. 16. T_2-store-T_2 spectra of saturated sucrose in D_2O acquired at 23.4 MHz with a CPMG pulse spacing of 200 μs and store times of (a) 200 μs; (b) 500 μs (c) 2 ms; (d) 40 ms.

Fig. 6a are arrayed along the diagonal but even at this short store time there are hints of cross-peaks CP_{24} and CP_{34}. Fig. 18b superimposes the cross-peaks appearing as the store time is increased and shows how the "exchange squares" do, in fact, emerge in the superposition. However, as Fig. 18b shows, not all cross-peaks appear at any particular store time. Peaks 2 and 3 are not well resolved so have been grouped together as "23" and CP_{14} shows large shifts with store time.

Replacing H_2O with D_2O increases the relative intensity of the sucrose on-exchanging CH peaks and reveals exchange cross-peaks between peaks 2 and 3 (see Fig. 19a). Additional cross-peaks appear as the store tie is increased and these are summarised in Fig. 19b. As before different cross-peaks appear at different store times but the superposition confirms the existence of the exchange squares.

6. Discussion

Despite the various manipulations of the T_1–T_2 and T_2-store-T_2 spectra presented in this paper, peak assignment is far from straightforward and different samples will require different protocols. As we have shown, with small molecules such as sucrose the most reliable way to assign the peaks is to acquire water-suppressed T_1–T_2 spectra on a high-field, high resolution NMR spectrometer. Fourier transformation of each echo in the CPMG sequence and then yields separate T_1–T_2 spectra for each chemical-shift resolved proton peak. Unfortunately even this approach may fail for a number of reasons. First the because of the dependence of the relaxation times on spectrometer frequency it may not be straightforward to compare the assignments derived on a high field, high resolution spectrometer with the peaks acquired on a low-resolution low-field spectrometer. A comparison of

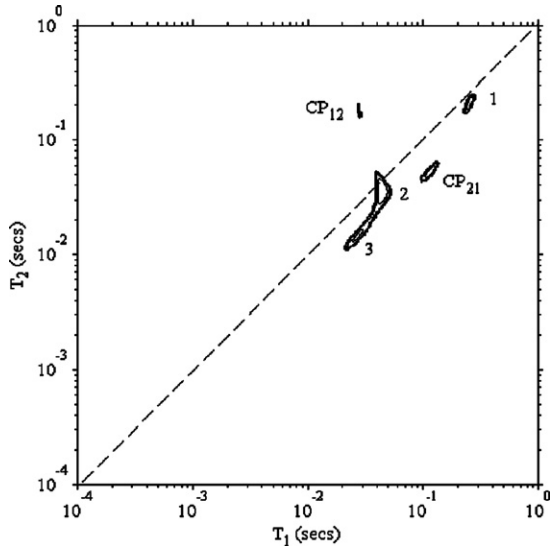

Fig. 17. T_1–T_2 spectra of saturated sucrose in D_2O acquired at 23.4 MHz with a CPMG pulse spacing of 200 μs.

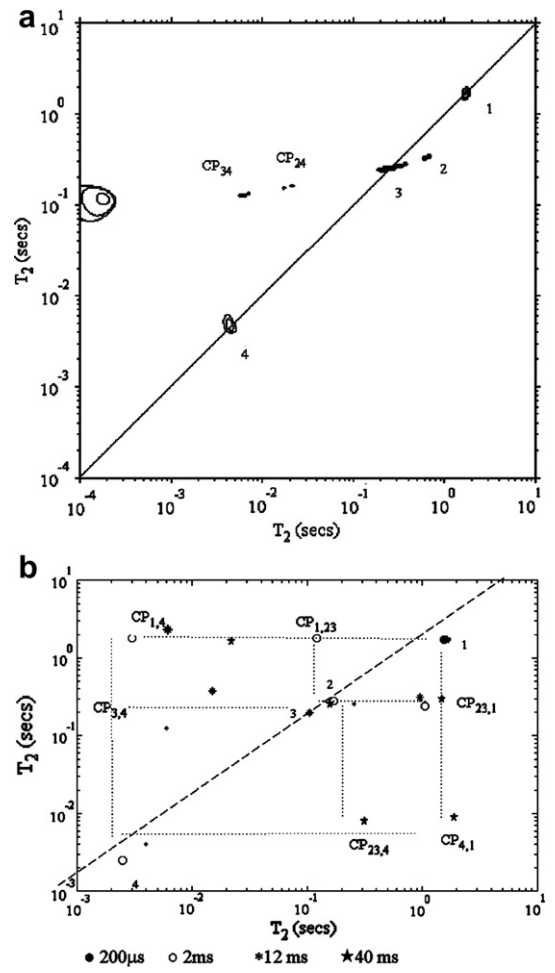

Fig. 18. T_2-store-T_2 spectra of 20% w/w sucrose in H_2O acquired at 23.4 MHz with a CPMG pulse spacing of 200 μs. (a) Spectrum with a store time of 250 μs. (b) A summary of the spectra for store times of 200 μs; 2 ms; 12 ms and 40 ms.

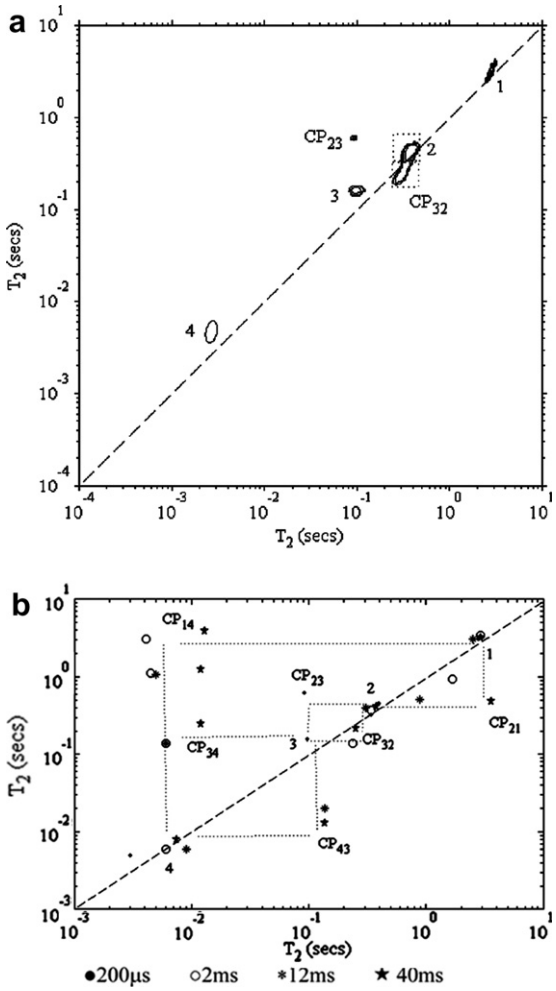

Fig. 19. T_2-store-T_2 spectra of 20% w/w sucrose in D_2O acquired at 23.4 MHz with a CPMG pulse spacing of 200 μs. (a) Spectrum with a store time of 250 μs. (b) A summary of the spectra for store times of 200 μs, 2 ms and 40 ms.

the spectra in Fig. 9a with 7a illustrates this difficulty. Secondly, it may not be possible to acquire a well-resolved high resolution spectrum on complex samples, especially the heterogeneous multicomponent, multiphase biopolymer systems of interest in the biosciences and the food industry. One must then resort to some of the other methods presented in this paper, such as the field-cycling and q-weighted T_1–T_2 techniques to try to assign peaks.

Even when these methods fail and peak assignment remains uncertain, T_1–T_2 spectra can be used empirically as a ''finger-print'' for monitoring, at the molecular and microscopic scale, the complex changes associated with phase transformations, aggregation, gelation and crystallisation. It is therefore anticipated that multidimensional relaxation and diffusion methods will therefore find important applications throughout food and materials science.

Acknowledgments

The authors wish to thank the BBSRC for funding support and L.Venturi thanks the University of Bologna for a MARCO POLO grant.

References

[1] B.P. Hills, Magnetic Resonance Imaging in Food Science, John Wiley, New York, 1998.
[2] Y.-Q. Song, L. Venkataramanan, M.D. Hurlimann, M. Flaum, P. Frulla, C. Straley, J. Magn. Reson. 154 (2002) 261.
[3] M.D. Hurlimann, L.J. Venkataramanan, J. Magn. Reson. 157 (2002) 31.
[4] S. Godefroy, L.K. Creamer, P.J. Watkinson and P.T. Callaghan, The use of 2D Laplace Inversion in Food Material, page 85 in Magnetic Resonance in Food Science,.
[5] M.D. Hurlimann, L. Burcaw, Y.-Q. Song, Colloid Interface Sci. 297 (2006) 303.
[6] B.P. Hills, S. Benamira, N. Marigheto, K.M. Wright, Applied Magn. Reson. 26 (2004) 543.
[7] N. Marigheto, K. Wright, B.P. Hills, Appl. Magn. Reson. 30 (2006) 13.
[8] B.P. Hills, A. Costa, N. Marigheto, K. Wright, Applied Magn. Reson. 28 (2005) 13.
[9] D. Girlich, H.-D. Ludemann, Zeitschrift fur Naturforschung 48c (1993) 407.
[10] S.B. Engelsen, C. Herve du Penhoat, S. Perez, J. Phys. Chem. 99 (1995) 13334.
[11] S. Sheng, H. van Halbeek, Biochem. Biophys. Res. Commun. 215 (1995) 504.
[12] S.B. Engelsen, S. Perez, J. Mol. Graph. Model. 15 (1997) 122.
[13] B.P. Hills, Y.L. Wang, H.-R. Tang, Mol. Phys. 19 (2001) 1679.
[14] B.P. Hills, K.M. Wright, P.S. Belton, Mol. Phys. 67 (1989) 1309.
[15] B.P. Hills, J.E.M. Snaar, Mol. Phys. 76 (1992) 979.
[16] M. Guillon-Charpin, D. LeBotlan, C. Tellier, B. Mechin, Sci. Aliment. 10 (1990) 377.
[17] P.J. McDonald, J.-P. Korb, J. Mitchell, L. Monteilhet, Phys. Rev. E 72 (2005) 011409.
[18] L. Monteilhet, J.-P. Korb, J. Mitchell, P.J. McDonald, Phys. Rev. E. 74 (2006) 061404.